Effects of Arylsulfatase B and Pembrolizumab in Combination

on Progression of Metastatic Melanoma in the B16F10 Syngeneic Mouse Model

Sumit Bhattacharyya[1,2]
Insug O-Sullivan[1,2]
Joanne Tobacman[1,2]

[1]Jesse Brown VA Medical Center, Chicago, IL and

[2]University of Illinois at Chicago, Chicago, IL

Correspondence to:
Joanne K. Tobacman, MD
820 S. Damen Ave. Room 7247
Chicago, IL 60612
Telephone: 312-569-7826
E-mail: jkt@uic.edu

ABSTRACT

In this report, experiments were performed to assess how Arylsulfatase B (ARSB; N-acetylgalactosamine-4-sulfatase) treatment might interact with Pembrolizumab and improve therapeutic responses in melanoma. ARSB acts to remove 4-sulfate groups from chondroitin 4-sulfate (C4S; chondroitin sulfate A; CSA). ARSB is required for the degradation of CAS, an oncofetal, tumor-agnostic antigen. Previous reports showed that in syngeneic B16F10 mouse melanomas, ARSB inhibited progression of subcutaneous and metastatic pulmonary melanomas and improved survival. ARSB enhanced apoptosis, which was mediated by increased expression of Constitutive Photomorphogenic (COP)1, an E3 ubiquitin ligase. In this report, we show how treatment by recombinant human ARSB and Pembrolizumab lead to increased apoptosis, declines in expression of metalloproteinases MMP2 and MMP9 and in invasiveness, and altered cytokine/chemokine expression. The synergism between ARSB and Pembrolizumab may affect the progression of melanoma and improve treatment outcomes.

INTRODUCTION

The enzyme ARSB (Arylsulfatase B; N-acetylgalactosamine-4-sulfatase) removes 4-sulfate groups from N-acetylgalactosamine-4-sulfate, including 4-sulfate groups at the non-reducing end of chondroitin 4-sulfate (C4S; chondroitin sulfate A; CSA) and dermatan sulfate (DS). Congenital, inherited inactivating mutations of ARSB lead to the diffuse accumulation of these sulfated glycosaminoglycans in the lysosomal storage disorder Mucopolysaccharidosis (MPS) VI. MPS VI is characterized by organ dysfunction, respiratory insufficiency, skeletal deformities with short stature and cartilage abnormalities, and reduced life expectancy [1]. Treatment with rhARSB is effective and well-tolerated, leading to significant clinical improvement [2]. In multiple reports, we have shown that acquired decline in ARSB is associated with malignancy, including of colon, prostate, and breast, as well as melanoma [3-12]. Malignancy results from the disruption of normal intra- and intercellular signaling and leads to transcriptional events, mediated by epigenetic effects, activation of transcription factors, including AP-1, Sp1, Smad3, c-Myc, and MITF, and Wnt signaling [3,6,13-22]. ARSB is required for removal of the 4-sulfate group at the non-reducing end of C4S (CSA) and the subsequent degradation of C4S. C4S is also known as chondroitin sulfate A, and is recognized as an oncofetal antigen and the target of the malarial protein VAR2CSA [23-28].

The diverse signaling effects following decline in ARSB are attributable to increased sulfation and accumulation of C4S when ARSB activity declines, leading to changes in the extent of binding of critical molecules with C4S. Critical effects include reduced binding of galectin-3 with more sulfated C4S and increased binding of SHP2 (PTPN11), the ubiquitous non-receptor tyrosine phosphatase, with more sulfated C4S. Increased binding of SHP2 with C4S leads to sustained phosphorylation of vital signaling molecules, including phospho-p38 MAPK and phospho-ERK1/2, and profound disruption of intracellular signaling [3,6,14-22]. These findings demonstrate that decline in ARSB acts as a tumor promoter. Recent treatment studies with rhARSB in the B16F10 syngeneic melanoma model show that recombinant human ARSB acts as

a tumor suppressor, associated with improved survival, smaller and fewer subcutaneous tumors, and fewer pulmonary metastases [4-6].

This background indicates major effects of ARSB and C4S on melanoma cells, and suggests that combination with therapeutic agents, such as checkpoint inhibitors, that enhance the immune attack may be more effective than either approach alone. With consideration of the potential clinical role of rhARSB, additional studies were undertaken to examine how rhARSB and Pembrolizumab interact in the treatment of pulmonary melanomas in the B16F10 syngeneic model. Since treatment by ARSB reduced expression of PD-L1 [13], we anticipated that Pembrolizumab effectiveness would be enhanced in combination with ARSB. Experiments were performed to test how ARSB and Pembrolizumab in combination impacted on apoptosis, invasiveness, cytokine expression, and responses to peripheral blood mononuclear cells (PBMC), and polymorphonuclear leukocytes (PMN) in the syngeneic B16F10 pulmonary melanoma model and cell-based experiments.

RESULTS

Recombinant human (rh) ARSB and Pembrolizumab inhibit progression of metastatic pulmonary melanomas in the B16F10 syngeneic mouse model

Introduction of 250,000 B16F10 mouse melanoma cells by tail vein injection into 32 10.5-week-old male C57BL/6J mice produced pulmonary metastases in all of the experimental mice (**Fig.1A-1D**). A control group (n=7) was untreated and received normal saline IV on days 2,7, and 12 (**Fig.1A**). A second group (n=8) was treated by tail-vein injection of rhARSB 0.2 mg/kg (concentration of 50 µg/ml in normal saline) on days 2, 7, and 12 following tumor inoculation (**Fig.1B**). A third group (n=8) was treated by the anti-PD1 checkpoint inhibitor Pembrolizumab (5 mg/kg IP) on days 2,7, and 12 following tumor inoculation (**Fig.1C**). A fourth group (n=7) was treated by the combination of rhARSB (0.2 mg/kg IV) and Pembrolizumab (5 mg/kg IP) on days 2, 7, and 12 (**Fig.1D**). Comparison of the lung images indicates that the untreated mice had many more metastatic tumors than the treated mice. Tumors were quantified by unblinded observers, and the rhARSB-treated mice had the fewest tumors (**Fig.1E**). All treatment groups had fewer metastases than the saline-treated controls. One untreated mouse had macroscopic liver metastases, and one control and one combined treatment mouse died spontaneously days prior to termination of the study on day 14. These findings are consistent with previous reports that treatment by rhARSB reduced the size and increased the survival of mice with B16F10 subcutaneous melanomas [5] and reduced the number of pulmonary metastases in female mice with B16F10 syngeneic melanomas [4]. Additional experiments show that treatment by rhARSB inhibited development of A375 subcutaneous tumors in humanized NSG mice with PBMC implants (**Supplementary Fig. 1A**) and reduced the growth of B16F10 subcutaneous melanomas which were measureable prior to treatment (**Supplementary Fig. 1B**). No harmful effects of rhARSB or Pembrolizumab were observed in the treated mice.

Synergism between rhARSB and Pembrolizumab increases cleaved caspase-3 and reduces BCL2

Decline in pulmonary melanoma metastases following rhARSB was attributed to apoptosis, mediated by the E3 ubiquitin ligase constitutive photomorphogenic 1 (COP1) and the associated decline in BCL2 [4]. Here, combined treatment by rhARSB and Pembrolizumab leads to greater increase in cleaved caspase-3 than either agent alone ($p=1.2x10^{-7}$; unpaired t-test, two-tailed, unequal variation) (**Fig.2A**). COP1 expression is increased by rhARSB, but Pembrolizumab has no effect on COP1 expression (**Fig.2B**). Both rhARSB and Pembrolizumab reduce BCL2 expression, and their combination further reduces Bcl2 in the pulmonary melanomas ($p = 3.5 x 10^{-6}$) (**Fig.2C**). The Spearman correlation coefficient between BCL2 and cleaved caspase-3 is -0.97, reflecting the impact of BCL2 (**Fig.2D**). Correlation coefficient of COP1 and cleaved caspase-3 is 0.85 (**Fig.2E**), reflecting the impact of rhARSB these measurements.

In cultured A375 human melanoma cells treated with rhARSB, Pembrolizumab, peripheral blood mononuclear cells (PBMC), activated PBMC [PBMC(Ac)], and their combinations, cleaved caspase-3 increased following rhARSB ($p=1.4x10^{-8}$) or Pembrolizumab with activated PBMC ($p=2.7x10^{-9}$), but not by Pembrolizumab alone or Pembro with unactivated PBMC (**Fig.2F**). Cleaved caspase-3 increased more by rhARSB with activated PBMC ($p=7.8x10^{-7}$) than by rhARSB alone, and increased most by the combination of rhARSB, Pembrolizumab, and activated PMBC ($p = 1.9 x 10^{-13}$). RhARSB increased COP1 expression ($p=4.5x10^{-6}$), and COP1 expression was not increased by Pembrolizumab or increased further by the combination of rhARSB or Pembrolizumab and activated PBMC (**Fig.2G**). These findings demonstrate a requirement for activated PBMC for Pembrolizumab-induced apoptosis and confirm the lack of impact of Pembrolizumab on COP1 expression.

In contrast, to the lack of impact following Pembrolizumab and activated PBMC on COP1, rhARSB alone ($p=0.0005$) and Pembrolizumab with activated PBMC reduced BCL2 expression ($p=0.0009$). The combination of rhARSB, Pembroliziumab and activated PBMC reduced BCL2 mRNA expression by about 80% compared to control (**Fig.2H**). Both rhARSB and Pembrolizumab with activated PBMC increased granzyme in the pulmonary melanoma tissue. Granzyme B

increases apoptosis by BCL2-associated effects, and the increases in granzyme B reflect involvement of antitumor immune cells in Pembrolizumab-induced apoptosis in melanoma [29-33]. The combination of rhARSB, Pembrolizumab, and activated PBMC showed a synergistic increase in granzyme B ($p=2.8x10^{-6}$) (**Fig.2I**). These experiments indicate distinct mechanisms of BCL2 inhibition by rhARSB, mediated by COP1 and by granzyme-induced effects in the presence of activated PBMC. In contrast, Pembrolizumab had no effect on COP1, but had a greater effect on granzyme in the presence of activated PBMC than rhARSB and activated PBMC. The increase in cleaved caspase-3 activity and the increased reduction in BCL2 expression by the combination of rhARSB with Pembrolizumab *in vivo* or with Pembrolizumab and activated PBMC *in vitro* suggest a potential synergistic treatment benefit of these therapies in combination due to different mechanisms, since COP1 is not modified by Pembrolizumab and activated PBMC. These findings indicate that both the COP1- and the granzyme-mediated pathways can contribute to apoptosis by cleaved caspase-3 following rhARSB.

Exogenous ARSB reduces expression of matrix metalloproteinases (MMP) 2 and 9 in melanoma models

In addition to effects of rhARSB on apoptosis in melanoma, rhARSB also reduces the expression of matrix metalloproteinases 2 and 9, two Type IV gelatinases, which remodel the extracellular matrix to facilitate spread of malignant cells and are increased when ARSB is reduced [3,5,6,34,35]. In the pulmonary melanoma metastases, MMP2 and MMP9 expression declined significantly following rhARSB ($p=4.3x10^{-8}$, $p=0.00012$, respectively) (**Fig.3A,3B**). Pembrolizumab had no effect on expression of MMP9 or MMP2 in the melanoma tissue. The circulating level of MMP2 declined ~50% from baseline following rhARSB, declined ~19% following Pembrolizumab, and had greatest decline (~58%) by their combination (**Fig.3C**).

In A375 melanoma cells, rhARSB reduced MMP activity, ARSB siRNA increased MMP activity, and Pembrolizumab had no effect (**Fig.3D**). Consistent with these effects on activity, MMP2 (**Fig.3E**) and MMP9 (**Fig.3F**) expression declined following rhARSB and Pembrolizumab

had no effect. The addition of inactivated or activated PBMC had no impact on the MMP expression. Migration of the A375 cells declined following rhARSB, increased when ARSB was silenced, and was unaffected by Pembrolizumab (**Fig.3G**).

The impact of ARSB on MMP expression is mediated by a signaling pathway attributable to effects of decline in ARSB on chondroitin 4-sulfation, leading to increased binding of chondroitin 4-sulfate (C4S) with SHP2, the ubiquitous non-receptor tyrosine phosphatase, as previously detailed in human melanoma cell lines, subcutaneous melanomas, and other tissues [3-6]. These mechanisms are presented in A375 cells (**Supplementary Fig. 2A-G**). Also, in normal melanocytes, ARSB siRNA increased MMP2 expression (**Supplementary Fig. 3A**) and in B16F10 mouse melanoma cells rhARSB reduced MMP2 and MMP9 expression and ARSB siRNA increased MMP expression, with greater increase in MMP2 than MMP9 (**Supplementary Fig. 3B**).

Cytokine expression following rhARSB, Pembrolizumab, and their combination in pulmonary melanomas

In the B16F10 pulmonary melanomas, combined treatment by rhARSB and Pembrolizumab produced greater increases in MCP1 and IL-10 mRNA expression than either agent alone (**Fig.4A**). In contrast, IL-17α was increased by Pembrolizumab, but ARSB had no effect. Combined treatment produced greater declines in KC, the mouse analog of IL-8, and IL-6 than either agent alone (**Fig.4B**). Overall, there was decline in TNFα due to the inhibitory effect of rhARSB, but, in contrast, Pembrolizumab alone increased TNF-α. Declines in bFGF, VEGF, and EGF followed rhARSB treatment, and Pembrolizumab had no impact on these declines (**Fig.4C**)**.** The impact of ARSB silencing and exogenous rhARSB on cytokine expression by A375 cells is shown in a cytokine array and was confirmed by mRNA data (**Supplementary Fig.4**).

Impact of rhARSB and chondroitin 4-sulfate - IL-8 interaction on polymorphonuclear leukocyte (PMN) invasion and apoptosis

PMN invasion to A375 cells was measured by a two-cell layer culture experiment in which A375 cells were plated on the bottom surface of transwells and calcein-labeled neutrophils were introduced into the filter on top. Their passage through the filter was quantified by detection of calcein fluorescence in the lower compartment. Following rhARSB treatment of A375 cells or by addition of exogenous rh IL-8 (**Fig.5A**), PMN migration increased. Inversely, silencing ARSB in the A375 cells (**Fig.5A**) reduced the PMN invasion. Pembrolizumab alone had no impact on PMN migration (**Fig.5B**). To evaluate how ARSB mediated the increase in PMN migration to the A375 cells, the impact of rhARSB and of ARSB siRNA on IL-8 in the cell extract, spent media and total was determined. IL-8 in the spent media increased following rhARSB (**Fig.5C**), leading to increased PMN invasion. In contrast, the IL-8 associated with the A375 cell extract declined following rhARSB and increased following ARSB siRNA (**Fig.5C**). These effects are attributable to increased binding of IL-8 to the more highly sulfated chondroitin 4-sulfate of the A375 cells which is present when ARSB activity is less (**Supplementary Fig.5A,5B**). In contrast, chondroitin 6-sulfate did not bind with IL-8 (**Supplementary Fig. 5C**).

When A375 cells were treated by rhARSB, Pembrolizumab and activated PBMC, the effect of activated PBMC on cleaved caspase-3 was significantly reduced by knockdown of IL-8 (**Fig.5D**). Cleaved caspase-3 was increased by the addition of neutrophils following treatment by rhARSB, Pembrolizumab and activated PBMC (**Fig.5E**).

Discussion

Metastatic malignant melanoma remains a devastating disease and advances in treatment options have the potential to improve quality of life and survival for thousands of patients. With this objective, the current studies have addressed the potential benefits of treatment by rhARSB, Pembrolizumab, and their combination in human cell-based and murine *in vivo* studies. The combined effects of rhARSB and Pembrolizumab demonstrate synergism, which may be of significant clinical benefit. Enhanced apoptosis mediated by different Bcl2 regulatory mechanisms, decline in matrix metalloproteinases and invasiveness, and effects on cytokine expression are anticipated to inhibit melanoma progression. Although no particular advantage was shown in the pulmonary B16F10 syngeneic metastatic melanoma model, the effects on apoptosis, invasiveness, and cytokine expression suggest that the application of modified, combined dosing regimens will lead to enhanced therapeutic benefit.

Interest in the role of chondroitin 4-sulfate (C4S; chondroitin sulfate A; CSA) as a tumor-agnostic, oncofetal antigen reflects the underlying significance of ARSB, since ARSB is the specific chondroitin sulfatase enzyme that removes 4-sulfate groups from the non-reducing end of C4S and is required for the degradation of C4S, as evident in MPS VI [1,2,23-28]. The malarial protein VAR2CSA of plasmodial-infected erythrocytes attaches to the more highly C4S present in the placenta and in small extracellular vesicles associated with adenocarcinoma [28]. These associations are consistent with the impact of ARSB on chondroitin 4-sulfation and the reported effect of the anti-malarial drug chloroquine on the inhibition of ARSB activity [34].

Investigations have shown that activity and/or expression of ARSB is regulated by several potential conditions or exposures [3,12,16, 34-44]. These include: decline in the cystic fibrosis transmembrane regulator (CFTR) in cystic fibrosis, high chloride, high phosphate, low oxygen, chloroquine, ethanol, carrageenan, estrogen, dihydrotestosterone, and COVID-19. Experiments have indicated that expression of ARSB may be influenced by Rb activation, as mediated by E2F1, phospho-p38α, and cyclin-induced phosphorylation of Rb [44]. Also, decline in ARSB, both

in MPS VI and in human hepatic cells and tissue from ARSB-null mice, is associated with mitochondrial abnormalities [45,46]. These include the presence of unusual inclusions and the disruption of normal mitochondrial function, consistent with impaired aerobic metabolism. The overlap between effects of decline in ARSB and of hypoxia is consistent with an oxygen requirement for the post-translational modification of ARSB by the formylglycine modifying enzyme (FGE), encoded by SUMF (sulfatase modifying factor) [47,48]. Also, decline in ARSB gene expression was reported in association with unresponsiveness of patients with moderate COPD to oxygen therapy [49].

Several signaling mechanisms by which ARSB independently can affect progression of melanoma and potentially other malignancies have been published [13-22]. These mechanisms are predominantly dependent on ARSB mediated changes in chondroitin 4-sulfation and the consequent impact on binding with critical signaling molecules, including galectin-3 and SHP2. When ARSB activity is reduced, chondroitin 4-sulfation is increased, and binding of galectin-3 with C4S is reduced. This increases the availability of galectin-3 to influence transcriptional events by enhanced effects of transcription factors, including AP-1 and Sp1. We have shown that increase in free galectin-3 following decline in ARSB enables increased expression of HIF-1α, versican, CSPG4, and Wnt9A, and PD-L1 by an HDAC3-mediated epigenetic mechanism [5,6,13,15,16,18].

In contrast to reduced binding of galectin-3 with more highly sulfated C4S, the ubiquitous non-membrane tyrosine phosphatase SHP2 (PTPN11), binds more with C4S when ARSB activity is reduced. Signaling effects when SHP2 is bound more with C4S involve extensive persistent phosphorylations with sustained activation of important, diverse mediators. Ser-Thr phosphorylations are influenced through effects on Tyr-Thr phosphorylation sites on phospho-p38, ERK1/2, and JNK. These changes affect transcription factors, including c-Myc, MITF, c-jun, and c-fos and expression of MMP2, MMP9, GPNMB, EGFR, and DNMT with subsequent impact on methylation of the DKK3 promoter and activation of Wnt/β-catenin signaling [5,6,14,17,18-22].

Additional impact of decline or increase in ARSB activity is attributable to altered binding of more or less sulfated C4S and interactions with other molecules. We have reported increased binding of IL-8, BMP4, and kininogen with C4S when ARSB is reduced [20,39,50]. Increased binding of IL-8 with C4S may affect the attraction or adherence of neutrophils or circulating mononuclear cells to malignant cells. The increased migration of neutrophils toward the A375 cells in experiments in this report is consistent with the impact of increased IL-8 secretion when ARSB is reduced and IL-8 binds more tightly with C4S (**Supplementary Fig.5**). Also, enhanced binding of BMP4 when ARSB is lower and chondroitin 4-sulfation is increased leads to reduced nuclear phospho-Smad3 and reduced chondroitin 4-sulfotransferase (CHST11) expression, providing a feedback mechanism by which increased C4S may regulate its own production [20].

The chondroitin 4-sulfate (C4S) sulfatase Arylsulfatase B (ARSB; N-acetylgalactosamine-4-sulfatase) inhibits growth and improves survival of C57BL/6J mice with B16F10 subcutaneous melanomas, inhibits growth of A375 human melanomas in humanized mice with PBMC implants, and reduces the progression of metastatic pulmonary melanomas in the B16F10 syngeneic mouse model. Cleaved caspase-3 is enhanced by treatment with rhARSB and is mediated by increased expression of the E3 ubiquitin ligase constitutive photomorphogenic (COP)1, which reduces nuclear ETS-1 and thereby BCL2 expression. Combined treatment of B16F10 pulmonary melanomas by rhARSB and Pembrolizumab leads to greater increase in cleaved caspase-3 and greater decline in Bcl2, but no further increase in COP1, than by rhARSB alone. Similarly, in cultured A375 cells, cleaved caspase-3 is increased and BCL2 is reduced further by combined treatment of rhARSB and Pembrolizumab in the presence of PBMC, without further increase in COP1 than by rhARSB alone. The greater decline in Bcl2 is attributable to effects of rhARSB and Pembrolizumab in the presence of PBMC on Granzyme B. ARSB and Pembrolizumab reduce expression of the matrix metalloproteinases MMP2 and MMP9 in A375 melanoma cells and in B16F10 pulmonary melanomas, which are anticipated to lead to decline in tumor invasiveness. In the B16F10 pulmonary melanomas, the combination of Pembrolizumab and rhARSB increases

the mRNA expression of MCP1 and IL-10 and reduces the expression of KC and IL-6, more than either treatment alone. ARSB alone increases IL-17α and TNFα; however, TNFα is reduced by Pembrolizumab and overall by the combination. The studies in this report are considered as evidence of how combined treatments, one directed at enhancing the cytotoxic T-cell response in the tumor microenvironment and the other at modulating intracellular signaling events and expression of critical signaling molecules, may together lead to more effective treatment of malignant melanoma and improved survival.

MATERIALS AND METHODS

Syngeneic B16F10 pulmonary melanomas in C57BL/6J mice

Eight-week-old male C57BL/6J mice (n=32) were purchased (Jackson Laboratories, Bar Harbor, Maine) and housed in the Veterinary Medicine Unit at the Jesse Brown Veterans Affairs Medical Center (JBVAMC, Chicago, IL). Principles of laboratory animal care were observed, and all procedures were approved by the AALAC accredited Animal Care Committee of the JBVAMC. Mice were fed a standard diet and maintained in groups of four in a cage with routine light–dark cycles, as previously [4,5]. Mice were ear-punched for identification and divided into four groups, which were inoculated with 250,000 B16F10 tumor cells in saline by tail vein injection on day 0. B16 F10 cells were cultured in DMEM (ATCC 30-2002) with 10% FBS under the recommended conditions. Recombinant bioactive ARSB (R&D Systems, Bio-Techne, Minneapolis, MN) at a dose of 0.2 mg/kg BW in normal saline was injected into the tail vein. Eight untreated mice received parallel vehicle (saline) injections. Pembrolizumab was purchased (MedChemExpress, Mammoth Junction, NJ) and injected intraperitoneally at a concentration of 5 mg/kg. Treatment groups included: rhARSB-treated (0.2 mg/kg IV on days 2, 7, 12); Pembrolizumab (5 mg/kg IP on days 2, 7, and 12); and combined Pembrolizumab (5 mg/kg IP and rhARSB IV on days 2, 7, 12). Two mice died spontaneously of uncertain cause prior to day 14, including an untreated mouse on day 2 and a mouse with combined treatment on day 12. 30 mice were euthanized on day 14 by isoflurane inhalation and decapitation. At the time of euthanasia, lung, liver, spleen, blood, and other organs were harvested. Pulmonary nodules were counted by two observers and photographed.

Cell culture of A375 melanoma cells and normal human melanocytes

A375 human melanoma cells (CRL-1619, ATCC, Manassas, VA) were grown in Dulbecco's modified Eagle medium (DMEM) with 10% fetal bovine serum (FBS; ATCC) and 1x penicillin-streptomycin (ATCC). Cells were maintained at 37°C in a humidified, 5% CO_2 environment with media exchange every 2 days. Confluent cells in T-25 flasks were harvested

using EDTA-trypsin (ATCC) and sub-cultured. Cells were screened for pathogens by IDEXX BioAnalytics (Columbia, MO).

Silencing of insulin-like growth factor 2 receptor (IGF2R), N-acetylgalactosamine-4-sulfatase (Arylsulfatase B, ARSB) and Interleukin (IL)-8 by siRNA

The mRNA expression of IGF2R and ARSB was silenced by specific siRNA using previously reported procedures [4-6,13]. Small interfering (si) RNA for IGF2R (Assay ID s7218, Thermo Fisher Scientific, Waltham, MA) and siRNA for ARSB siRNA were previously detailed [13,15]. Validated IL-8 (CXCL8) siRNA (Assay ID s7327, Thermo Fisher) was used with similar procedures. A375 cells were grown to ~70 % confluence, then silenced by adding 0.6 µl of 20 µM siRNA (150 ng), mixed with 100 µl of serum-free medium and 12 µl of HiPerfect Transfection Reagent (Qiagen, Germantown, MD). Media were changed after 24 h, and cell treatments were initiated.

Treatment of A375 human melanoma and melanocytes cells by exogenous ARSB and other agents

Cells were treated by exogenous, bioactive rhARSB (1 ng/ml x 24 h; R&D, Bio-Techne, Minneapolis, MN) for 24 h, unless indicated otherwise. Cells were treated with ERK activation inhibitor peptide 1, cell-permeable (10 µM; Sigma-Aldrich, Inc., St. Louis, MO); F4, a cell-permeable thiazolidinone compound which inhibits c-Myc-Max dimerization (64 µM, 10058-F4, Tocris Bioscience, Bio-Techne); and p38 MAPK inhibitor SB203580 (10 µM; Tocris Bioscience, Bio-Techne). Some preparations were treated with recombinant, human IL-8 (CXCL8 (1 ng/ml x 24h, 208-1L, R&D Systems).

ELISAs for cleaved caspase-3 (Asp175), IL-8, MMP2, and Granzyme B

Cleaved caspase 3 in the cell extracts was measured by a commercial sandwich duoset ELISA (DYC835, R&D Systems), following the instructions. Samples and standards were added to the wells of a microtiter plate precoated with a capture antibody. Cleaved caspase 3 in the cell extracts was captured by the coated antibody on the plate and detected with a biotinylated second

antibody to cleaved caspase 3. Streptavidin-HRP and hydrogen peroxide / tetramethylbenzidine (TMB) substrate were used to develop color proportional to the bound HRP activity. Similar ELISA procedures were used to quantify mouse matrix metalloproteinase (MMP)2 (ELM-MMP2, RayBiotech, Peachtree Corners, GA, USA), IL-8 (DY208, R&D Systems), IL-8 (DY208, R&D Systems), and Granzyme B (DY2906, R&D Systems). Results are reported as pg/mg protein, pg/ml or % control.

QRT-PCR for COP1, BCL2, MMP2, MMP9, MCP1, IL-10, IL-17α, KC, IL-6, TNFα, bFGF, VEGF, and EGF

Total RNA was prepared from treated and control cells or tissue using an RNeasy Mini Kit (Qiagen). Equal amounts of purified RNAs from the control and treated preparations were reverse-transcribed and amplified using Brilliant SYBR Green QRT-PCR Master Mix (Bio-Rad, Hercules, CA). Human β-actin was used as an internal control. QRT-PCR was performed using the following specific primers:

Human β-actin (NM_001101) left: 5'-CACCATTGGCAATGAGCGGTTC-3' and right: 5'-AGGTCDTTTGCGGATGTCCACGT-3';

Human BCL2 (NM_000633) left 5′-ATCGCCCTGTGGATGACTGAGT-3′ and right 5′-GCCAGGAGAAATCAAACAGAGGC-3′;

Human COP1 (NM_022457) left 5′-GTCAGTGAGGATAGCACAGTGC-3' and right 5′-GAGAACTGCCACTGAAACCTGG-3';

Human EGF (NM_001963) left 5'- TGCGATGCCAAGCAGTCTGTGA-3' and right 5'-GCATAGCCCAATCTGAGAACCAC;

Human FGF2 (NM_002006) left 5'- AGCGGCTGTACTGCAAAAACGG-3' and right 5'-CCTTTGATAGACACAACTCCTCTC;

Human IL-6 (NM_000600) left: 5'-AAAGCAGCAAAGAGGCACTG-3' and right 5'-TTTTCACCAGGCAAGTCTCC-3';

Human IL-8 (NM_00584) left:5'-GAGAGTGATTGAGAGTGGACCAC-3' and right 5'-CACAACCCTCTGCACCCAGTTT-3';

Human IL10 (NM_000572) left 5'-TCTCCGAGATGCCTTCAGCAGA-3' and right 5'-TCAGACAAGGCTTGGCAACCCA;

Human IL-17a (NM_002190) left 5'- CGGACTGTGATGGTCAACCTGA-3' and right 5'-GCACTTTGCCTCCCAGATCACA;

Human MCP1 (NM_002982) left 5'-GAGATCACCAGCAGCAAGGTGCC-3' and right 5'-TCCTGAACCCACTTCTGCTTGG-3';

Human MMP2 (NM_004530) left: 5′-AGTGGATGATGCCTTTGCTC-3′ and right: 5′-GAGTCCGTCCTTACCGTCAA-3′;

Human MMP9 (NM_004994.2) left: 5′-GTCTTCCCCTTCACTTTCCTG-3′ and right: 5′-TCAGTGAAGCG GTACATAGGG-3′;

Human TNFα (NM_000594) left 5'- CTCTTCTGCCTGCTGCACTTTG and right 5'-ATGGGCTACAGGCTTGTCACTC

Human VEGFA (NM_001025366) left 5'- TTGCCTTGCTGCTCTACCTCCA and right 5'-GATGGCAGTAGCTGCGCTGATA-3';

Mouse β-actin (NM_007393) left: 5'-CATTGCTGACAGGATGCAGAAGG-3' and right: 5'-TGCTGGAAGGTGGACAGTGAGG-3';

Mouse BCL2 (NM_009741) left: 5′-CCTGTGGATTGAGTACCTG-3′ and right 5′-AGCCAGGAGAAATCAAACAGAGG-3′;

Mouse COP1 (NM_011931) left: 5′-GCCTCTACTCTCTCAGTGA -3′ and right: 5′-GTCCCACTGAAACCTGGAGGTT-3′;

Mouse EGF (NM_010415) left 5'- GAGTTCCGTACTCCCTCTTGCA and right 5'-CAGCCAAGACTGTAGTGTGGTC-3';

Mouse bFGF (NM_008006) left 5'- AAGCGGCTCTACTGCAAGAACG-3' and right 5'-CCTTGATAGACACAACTCCTCTC-3';

Mouse IL6 (NM_031168) left 5'-AGTTGCCTTCTTGGGACTGA-3' and right 5'-TCCACGATTTCCCAGAGAAC-3';

Mouse IL-10 (NM_010548) left 5'-CGGGAAGACAATAACTGCACCC-3' and right 5'-CGGTTAGCAGTATGTTGTCCAGC-3';

Mouse IL-17a (NM_010552) left 5'- CAGACTACCTCAACCGTTCCAC-3' and right 5'-TCCAGCTTTCCCTCCGCATTGA-3';

Mouse KC (NM_008176) left 5'- TCCAGAGCTTGAAGGTGTTGCC-3' and right 5'-AACCAAGGGAGCTTCAGGGTC-3';

Mouse MCP1 (NM_011333.3) left 5'-ATCTGCCCTAAGGTCTTCAGC-3' and right 5'-TAAGGCATCACAGTCCGAGTC-3'.

Mouse MMP2 (NM_008610) left 5'-CAGTGATGGCTTCTTGTGGT-3' and right 5'-GGTCATAGTCCTCGGTGGTG-3';

Mouse MMP9 (NM_0113599.5) left 5'-GACTACGATAAGGACGGCAAA-3' and right 5'-CTCAAAGATGAACGGGAACAC-3';

Mouse VEGF (NM_001025250) left 5'- for CTGCTGTAACGATGAAGCCCTG-3' and right 5'-GCTGTAGGAAGCTCATCTCTCC-3'.

Cycle threshold (Ct) was determined during the exponential phase of amplification, as previously [15]. Fold changes in expression were determined by the difference between the Ct values of the gene of interest and the control.

Transcription Factor filter plate assay for c-Myc by DNA hybridization

Transcription Factor (TF) Filter Plate Assay kit and specific labeled DNA probe for c-Myc were obtained (Signosis, Santa Clara, CA). Nuclear extracts were obtained from treated and control cells and were mixed with a specific biotin-labeled c-Myc DNA binding sequence and TF-DNA complexes formed. The assay filter plate retained the bound DNA probe and free probe was removed. The bound, pre-labeled DNA probe was then eluted from the filter and collected for detection by streptavidin-HRP and quantitative analysis. Luminescence was reported as relative

light units (RLUs) on a microplate reader (FLUOstar, BMG Labtech, Cary, NC). The luminescence was normalized by total protein of the nuclear extract and expressed as percentage of control.

A375 migration assay

Invasiveness of A375 human melanoma cells was detected using a fluorescent cell invasion assay (QCM™ ECMatrix cell invasion assay (Millipore Sigma, Burlington, MA). A 96-well cell culture plate and cell culture inserts with 8 μm pores in a polycarbonate membrane and coated with a thin, dried layer of ECMatrix™ to block non-invasive cell migration, were used. A375 melanoma cells migrated through the ECM layer and attached to the bottom of the polycarbonate membrane. The cells were dissociated from the membrane by incubation with Cell Detachment Buffer. Then, the migrated cells were lysed and detected by a green-fluorescent dye (CyQuant GR dye, Thermo Fisher Scientific) using a fluorescence plate reader (BMG Labtech)..

Polymorphonuclear Leukocyte invasion assay

Human polymorphonuclear (PMN) cells (SER-PMN, PMN 042324B Blue 34/4 #65) were procured (Zenbio, Durham, NC). 350 μl of frozen cells containing about 5.25 x 10^6 million cells were thawed and washed twice with normal saline and then resuspended in 2.5 ml DMEM containing 10% FBS. Calcein-AM (5 μg/ml; Sigma-Aldrich) was added to the 2.5 ml suspension of cells in DMEM-FBS, and the cells were incubated for 30 min at 37°C. PMN were washed twice with normal saline, counted in a counting chamber, and resuspended in DMEM-FBS to the desired concentration of 2,000 cells/μl. To assess migration of the PMN to melanoma cells, 200,000 A375 cells were seeded into twenty-four well plates and treated with either rhARSB or silencing RNAs (ARSB and control) for 24 h. Disposable 24-well transwell filter inserts were placed inside each well (Corning, Thermo Fisher #07-200-174). The inserts for the 24-well plate were 6.5 mm in diameter, with culture area of 0.33 cm^2, and with pore size of 8 μm. 100 μl PMN suspensions were added directly onto the filters in each well, and the plate was incubated for 1 h (37°C and 5% CO_2). The non-migrating cells on the top of the filter were removed gently. The cells that migrated

into the bottom chamber were detected and measured by using the calcein fluorescence signal (excitation at 485 nm; emission at 530 nm) in a fluorescent plate reader (BMG Labtech).

Co-culture of PBMCs and PMNs with A375 Melanoma cells

A total of 10^5 A375 melanoma cells/well were seeded into twenty-four well plates in routine growth media, and siRNA for ARSB or control was added to some of the wells. After 24 h, media was removed and replenished with fresh media with or without ARSB (1 ng/ml). In some wells, 10^5 PBMCs (activated or non-activated), 10^5 PMN, or Pembrolizumab 2 ug/ml, either alone or in combination with other treatments, was added. PBMC were activated by treatment with anti-CD3 (10 µg; 16-0037-81, Invitrogen, Thermo Fisher) and anti-CD28 (10 µg, 16-0281-81, Invitrogen) to 10^6 PBMCs in10 ml of melanoma media in a T-25 flask. The cells were incubated with the antibodies at 37°C for 2 h for activation, and then were incubated for 24 h at 37°C and 5% CO_2. Then, the media was removed and saved, and the cells were washed with DPBS, and harvested by scraping.

Detection of IL-8 bound to chondroitin 4-sulfate

96-well ELISA plates were coated with 5 µg/ml of chondroitin 4-sulfate monoclonal antibody (Clone LY111, TCI, Portland, OR) or chondroitin 6-sulfate antibody (Clone MC21C, LSBio, Neward, CA) in PBS by adding 100 µl of antibody solution to each well and incubating at room temperature (RT) overnight. After antibody coating, the wells were washed three times with wash buffer (PBS 7.4 with 0.05% Tween 20) and blocked for 1 h at RT with Blocking Buffer (PBS 7.4 with 1% BSA). After blocking, 100 µl of chondroitin sulfate C (C6S) (2.5 µg/ml) from shark cartilage (predominantly C6S; Seikagaku, #400670, Tokyo, Japan; 73% 6S, 19 ± 1% 4S, 8% 2S6S, and 1% unsulfated chondroitin) or chondroitin sulfate A (C4S) (2.5 µg/ml) from bovine trachea (predominantly C4S; Sigma C9819; 86 ± 1% C4S, 12 ± 1% C6S, and 2% unsulfated chondroitin) was added to designated wells and incubated at 4°C overnight. Wells were washed three times with wash buffer, and 100 µl of recombinant human Interleukin-8 (208-IL, OriGene Technologies, Rockville, MD) at varying concentrations (20-1280 pg/ml) was added to specified

wells and incubated at RT for 2 h. Wells were washed, 100 µl of biotinylated IL-8 antibody (DY208, R&D) was added, and the plate was incubated at RT for 2 h. Subsequently, wells were washed three times, 100 µl of 1:200 Streptavidin-HRP was added in each well, and the plate was incubated at RT for 20 min. The color was developed by adding 100 µl of color reagent (1:1, H_2O_2:TMB), incubated for 15-20 min, and then the reaction was stopped by adding 50 µl of Stop Solution (2N H_2SO_4).. The optical density was measured at 450 nm in an ELISA plate reader (BMG Labtech).

MMP activity assay

Matrix metalloproteinase (MMP) activity was measured in the spent media of A375 cellls using the MMP activity assay (ab112146, Abcam, Cambridge, MA) in which a fluorescence resonance energy transfer (FRET) peptide is the MMP substrate. In the intact FRET peptide, the endogenous fluorescence of one part of the peptide is quenched by another part of the peptide. Following cleavage into two fragments by MMP, the fluorescence is recovered and can be detected in the fluorescence microplate reader (BMG Labtech) at Excitation/Emission = 490/525 nm. A375 melanoma cells were grown in 24-well clusters, and the FRET peptide was added when cells were ~70% confluent. Samples were incubated with an equal volume of 1 mM APMA (4-aminophenylmercuric acetate) at 37°C for 1 h (for MMP2) and green fluorescence measured.

Statistical analysis

The data presented in the Figures and Supplementary Figures are the mean ± SD of at least six independent experiments, unless indicated otherwise. Statistical significance of two-way comparisons was determined by unpaired, two-tailed *t*-tests with unequal standard deviations using Excel or Prizm (Version 10.3, GraphPad, CA) software, unless stated otherwise. Specific p-values are indicated for most of the comparisons with $p \leq 0.05$ considered significant. The data generated in this study are available from the corresponding author (JKT) upon request.

LEGENDS

Fig.1. Impact of ARSB and Pembrolizumab and their combination on pulmonary metastases in B16F10 melanoma

Thirty-two 10.5 week-old male C57BL/6J mice were inoculated with 250,000 B16F10 melanoma cells by tail vein injection. Two mice died of uncertain causes, and the remaining mice were euthanized on day 14 following tumor inoculation. Groups were:

A. untreated; **B.** rhARSB (0.2 ng/ml IV on days 2, 7, and 12); **C.** Pembrolizumab (5 mg/ml IP on days 2,7, and 12); and **D.** combined rhARSB and Pembrolizumab treatments.

E. Compared to saline-treated control, the rhARSB, Pembrolizumab, and the combined rhARSB and Pembrolizumab groups had significantly fewer tumors (unpaired t-test, two-tailed, unequal standard variation, $p<0.05$). Bar = 0.5 cm. (ARSB=arylsulfatase B=N-acetylgalactosamine-4-sulfatase; rh=recombinant human).

Fig.2. Effects of Pembrolizumab, ARSB, and their combination on COP1-mediated pathway of apoptosis in B16F10 pulmonary melanomas and A375 human melanoma cells

A. Cleaved caspase-3 increased following rhARSB ($p=2.5x10^{-7}$) or Pembrolizumab ($p=1.2x10^{-5}$) and was further Increased by their combination ($p=1.2x10^{-7}$) in treated B16F10 pulmonary melanomas. All p-values are calculated by unpaired t-test, two-sided with unequal standard deviation.

B. In treated B16F10 melanomas, COP1 mRNA expression increased following rhARSB, but not following Pembrolizumab treatment.

C. BCL2 mRNA expression declined following either rhARSB (p-1.7x10or Pembrolizumab and declined further by their combination in the B16F10 pulmonary melanomas.

D. Cleaved caspase-3 was inversely correlated with Bcl2 ($r = -0.97$; Spearman's correlation coefficient).

E. Cleaved capase-3 was directly correlated with COP1 in the pulmonary melanomas.($r=0.85$, Spearman's correlation coefficient).

F. In cultured human A375 melanoma cells, cleaved caspase-3 increased following rhARSB and was further increased by the combination of rhARSB with activated PBMC [PBMC(Ac)] (p=0.007). Pembrolizumab alone or Pembrolizumab with unactivated PBMC did not increase cleaved caspase-3. However, cleaved caspase 3 was increased by the combination of Pembrolizumab with PBMC(Ac) (p=0.002) and further increased by rhARSB, Pembrolizumab, and activated PBMC (p=0.009).

G. In the A375 cells, COP1 increased following rhARSB, but was unaffected by Pembrolizumab or by PBMC, either activated or not activated.

H. Inverse to the effect on COP1, rhARSB reduced the expression of BCL2. Neither Pembrolizumab alone nor PBMC alone affected BCL2 expression, but Pembro with activated PBMC reduced BCL2 ($p=4.1x10^{-5}$). BCL2 was further reduced by the combination of rhARSB + Pembrolizumab + PBMC(Ac) in the A375 cells ($p=4.8x10^{-9}$).

I. Granzyme B increased following the combinations of rhARSB and PBMC(Ac) ($p=5.3x10^{-10}$) and Pembrolizumab and PBMC(Ac) ($p=1.3x10^{-7}$). Synergistic effect was evident following treatment by rhARSB + Pembrolizumab + and PBMC(Ac) in the A375 cells.

[PBMC(Ac)=activated peripheral blood mononuclear cells; COP1=constitutive photomorphogenic protein 1; Pembro=Pembrolizumab; PBMC=peripheral blood mononuclear cells; rhARSB=recombinant human arylsulfatase B]

Fig.3. Matrix metalloproteinases following rhARSB and Pembrolizumab in B16F10 pulmonary metastatic melanomas and in A375 cells.

A,B. mRNA expression of MMP9 and MMP2 declined following rhARSB and was unchanged by Pembrolizumab.

C. Serum MMP2 declined more following rhARSB ($p=1.2x10^{-5}$) than following Pembroliziumab (p=0.004), and was further reduced by their combined treatment in mice with metastatic pulmonary melanomas.

D. Total MMP activity in spent media of A375 cells declined following rhARSB ($p=2.1x10^{-9}$), increased following ARSB siRNA ($p=3.2x10^{-10}$), but was unaffected by Pembrolizumab.

E,F. MMP2 and MMP9 mRNA expression in A375 cells was unaffected by Pembrolizumab, either alone or in combination with unactivated or activated PBMC. In contrast, rhARSB significantly reduced their expression.

G. Migration of A375 cells declined following rhARSB, increased following ARSB silencing, and was unaffected by Pembrolizumab**.**

[Ac=activated; ARSB=arylsulfatase B=N-acetylgalactosamine-4-sulfatase;MMP-matrix metalloproteinase; PBMC=peripheral blood mononuclear cells; Pembro=Pembrolizumab; rh=recombinant human; si=siRNA]

Fig.4. Expression of cytokines/chemokines in B16F10 melanoma lung tissue following rhARSB and Pembrolizumab

A. In B16F10 pulmonary melanoma tissue, mRNA expression of MCP1 and IL-10 increased following treatment by Pembrolizumab or rhARSB, and the increase was enhanced by their combination. In contrast, IL-17α expression was increased by Pembrolizumab, but not by rhARSB.

B. KC, the mouse analog of IL-8, and IL-6 were reduced by both rhARSB and Pembrolizumab and further reduced by their combination. In contrast, TNFα was increased by Pembrolizumab and reduced by rhARSB, with overall reduction by their combination.

C. FGF2, VEGF, and EGF were reduced by ARSB, but not by Pembrolizumab, and the combination of ARSB and Pembrolizumab did not lead to additional decline.

[ARSB=arylsulfatase B=N-acetylgalactosamine-4-sulfatase; EGF=epidermal growth factor; bFGF=basic fibroblast growth factor; IL=interleukin; KC=CXCL1=keratinocyte-derived cytokine; rh=recombinant human; MCP1=CCL2= monocyte chemoattractant protein-1; VEGF=vascular endothelial growth factor]

Fig.5. Effects of rhARSB and Pembrolizumab on polymorphonuclear (PMN) leukocyte invasion and apoptosis in A375 cells

A. Although KC expression was overall reduced by rhARSB in the mouse pulmonary metastases (**Fig.4B**), IL-8 in the spent media of A375 cells following ARSB increased ($p=2.5x10^{-5}$) and declined when ARSB was silenced ($p=2.5x10^{-5}$). In contrast, IL-8 in the cell extract declined following rhARSB declined following rhARSB ($p=1.1x10^{-7}$).

B. PMN invasion to the A375 cells was increased by rhARSB (p=0.0041), reduced by ARSB siRNA (p=0.0026), reduced by IL-8 silencing (p=0.00027), and increased by addition of rhIL-8 ($p=6.1x10^{-5}$). These effects are attributable to increased IL-8 in the spent media following rhARSB.

C. PMN migration from the filter on top to the bottom well was increased by IL-8 in the bottom well, but unaffected by Pembrolizumab.

D. When IL-8 was silenced in the A375 cells, the effect of rhARSB + PBMC(Ac) and of Pembro + PBMC(Ac) and their combination [rhARSB+Pembro+PBMC(Ac)] on cleaved caspase-3 was reduced, consistent with an effect of IL-8 on PBMC(Ac)-mediated apoptosis.

E. When PMN were added to the combination of rhARSB+Pembrolizumab+PBMC, the cleaved caspase-3 was further increased in the A375 cells (p=0.03).

[Ac=activated, consi=control siRNA; IL=interleukin; rh=recombinant human; Pembro=Pembrolizumab; PBMC=peripheral blood mononuclear cells; PMN=polymorphonuclear leukocytes; si=siRNA]

REFERENCES

1. Harmatz P, Shediac R. Mucopolysaccharidosis VI: pathophysiology, diagnosis and treatment. Front Biosci (Landmark Ed). 2017;22(3):385-406.
2. Burton BK, Harmatz PR, Horvathova V, Lail A, Lampe C, Parini R, Sharma R, Teles EL. Long-term enzyme replacement therapy: Findings from the mucopolysaccharidosis VI clinical surveillance program after 15 years follow-up. Mol Genet Metab. 2025;145(3):109135.
3. Tobacman JK, Bhattacharyya S. Profound impact of decline in N-acetylgalactosamine-4-sulfatase (Arylsulfatase B) on molecular pathophysiology and human diseases. Int J Mol Sci. 2022;23(21):13146.
4. Bhattacharyya S, O-Sullivan I, Whiteley HE, Yang J, Zhang F, Tobacman JK. Arylsulfatase B induces melanoma apoptosis by the ubiquitin ligase COP1. J Biol Chem. 2025;301(8):110402.
5. Bhattacharyya S, O-Sullivan I, Tu J, Chen Z, Tobacman JK. Exogenous recombinant N-acetylgalactosamine-4-sulfatase (Arylsulfatase B; ARSB) inhibits progression of B16F10 cutaneous melanomas and modulates cell signaling. Biochim Biophys Acta Mol Basis Dis. 2024;1870(1):166913. Erratum in: Biochim Biophys Acta Mol Basis Dis. 2024;1870(6):167231.
6. Bhattacharyya S, Feferman L, Terai K, Dudek AZ, Tobacman JK. Decline in arylsulfatase B leads to increased invasiveness of melanoma cells. Oncotarget 2017;8:4169–4180.
7. Feferman L, Deaton R, Bhattacharyya S, Xie H, Gann PH, Melamed J, Tobacman JK. Arylsulfatase B is reduced in prostate cancer recurrences. Cancer Biomark. 2017;12;21(1):229-234.
8. Feferman L, Bhattacharyya S, Deaton R, Gann P, Guzman G, Kajdacsy-Balla A, Tobacman JK. Arylsulfatase B (N-acetylgalactosamine-4-sulfatase): potential role as a biomarker in prostate cancer. Prostate Cancer Prostatic Dis 2013;16(3):277-284.
9. Bhattacharyya S, Tobacman JK. Arylsulfatase B regulates colonic epithelial cell migration by effects on MMP9 expression and RhoA activation. Clin Exp Metastasis 2009;26(6):535-545.
10. Prabhu SV, Bhattacharyya S, Guzman-Hartman G, Macias V, Kajdacsy-Balla A, Tobacman JK. Extra-lysosomal localization of arylsulfatase B in human colonic epithelium. J Histochem Cytochem 2011;59(3):328-335.
11. Bhattacharyya S, Kotlo K, Shukla S, Danziger RS, Tobacman JK. Distinct effects of N-acetylgalactosamine-4-sulfatase and galactose-6-sulfatase expression on chondroitin sulfate. J Biol Chem 2008;283(15):9523-9530.
12. Bhattacharyya S, Tobacman JK. Steroid sulfatase, arylsulfatases A and B, galactose 6-sulfatase, and iduronate sulfatase in mammary cells and effects of sulfated and non-sulfated estrogens on sulfatase activity. J Steroid Biochem Mol Biol 2007;103(1):20-34.
13. Bhattacharyya S, O-Sullivan I, Tobacman JK. N-Acetylgalactosamine-4-sulfatase (Arylsulfatase B) regulates PD-L1 expression in melanoma by an HDAC3-mediated epigenetic mechanism. Int J Mol Sci. 2024;25(11):5851.
14. Bhattacharyya S, Feferman L, Tobacman JK. Chondroitin sulfatases differentially regulate Wnt signaling in prostate stem cells and prostate cancer through effects on SHP2, phospho-ERK1/2, and Dickkopf wnt signaling pathway inhibitor (DKK3). Oncotarget. 2017;8(59):100242-100260.
15. Bhattacharyya S, Feferman L, Tobacman JK. Arylsulfatase B regulates versican expression by galectin-3 and AP-1 mediated transcriptional effects. Oncogene. 2014;33:5467-5476.
16. Bhattacharyya S, Tobacman JK. Hypoxia reduces arylsulfatase B activity and silencing arylsulfatase B replicates and mediates the effects of hypoxia. PLoS One. 2012;7(3): e33250.
17. Bhattacharyya S, Feferman L, Han X, Ouyang Y, Zhang F, Linhardt RJ, Tobacman JK. Decline in arylsulfatase B expression increases EGFR expression by inhibiting the protein-tyrosine phosphatase SHP2 and activating JNK in prostate cells. J Biol Chem. 2018;293(28):11076-11087.

18. Bhattacharyya S, Feferman L, Tobacman JK. Increased expression of colonic Wnt9A through Sp1-mediated transcriptional effects involving arylsulfatase B, chondroitin 4-sulfate, and galectin-3. J Biol Chem. 2014;289:17564-17575.
19. Bhattacharyya S, Feferman L, Han X, Xia K, Zhang F, Linhardt RJ, et al. Increased CHST15 follows decline in arylsulfatase B (ARSB) and disinhibition of non-canonical WNT signaling: potential impact on epithelial and mesenchymal identity. Oncotarget. 2020;11(24):2327-2344.
20. Bhattacharyya S, Feferman L, Tobacman JK. Regulation of chondroitin-4-sulfotransferase (CHST11) expression by opposing effects of arylsulfatase B on BMP4 and Wnt9A. BBA: Gene Reg Mech 2015;1849(3):342-352.
21. Bhattacharyya S, Feferman L, Tobacman JK. Inhibition of phosphatase activity follows decline in sulfatase activity and leads to transcriptional effects through sustained phosphorylation of transcription factor MITF. PLoS One. 2016;11:e0153463.
22. Bhattacharyya S, Feferman L, Tobacman JK. Dihydrotestosterone inhibits arylsulfatase B and Dickkopf Wnt signaling pathway inhibitor (DKK)-3 leading to enhanced Wnt signaling in prostate epithelium in response to stromal Wnt3A. Prostate. 2019;79(7):689-700.
23. Spliid CB, Toledo AG, Sanderson P, Mao Y, Gatto F, Gustavsson T, et al. The specificity of the malarial VAR2CSA protein for chondroitin sulfate depends on 4-O-sulfation and ligand accessibility. J Biol Chem. 2021;297(6):101391.
24. Vidal-Calvo EE, Martin-Salazar A, Choudhary S, Dagil R, Raghavan SSR, Duvnjak L, et al. Tumor-agnostic cancer therapy using antibodies targeting oncofetal chondroitin sulfate. Nat Commun. 2024;15(1):7553.
25. Rogerson SJ, Chaiyaroj SC, Ng K, Reeder JC, Brown GV. Chondroitin sulfate A is a cell surface receptor for Plasmodium falciparum-infected erythrocytes. J Exp Med. 1995;182(1):15-20.
26. Fried M, Duffy PE. Adherence of Plasmodium falciparum to chondroitin sulfate A in the human placenta. Science. 1996;272(5267):1502-4.
27. Dube Y, Hasang W, Teo A, Madanitsa M, Nielsen MA, Ter Kuile FO, et al. A high-throughput assay to measure antibodies that block adhesion of Plasmodium falciparum infected erythrocytes to chondroitin sulfate A. J Immunol Methods. 2025;545:114003.
28. Zhao Y, Wen C, Wang Q, Qing Y, Tondi S, Reina C, et al. Use of the Malaria Protein VAR2CSA for the detection of small extracellular vesicles to diagnose adenocarcinoma. J Extracell Vesicles. 2025;14(4):e70067.
29. Lord SJ, Rajotte RV, Korbutt GS, Chris BR. B. Granzyme, a natural born killer. Immunol Rev 2003;193:31-38.
30. Rousalova I, Krepela E. Granzyme B-induced apoptosis in cancer cells and its regulation (review). Int J Oncol. 2010;37(6):1361-78.
31. Lee J, Kim J, Sin JI. B16 melanomas evade antitumor immunity by the loss of epitope presentation and the acquisition of tumor resistance to granzyme B. Cell Immunol. 2021; 367:104394.
32. Waterhouse NJ, Sedelies KA, Trapani JA. Role of Bid-induced mitochondrial outer membrane permeabilization in granzyme B-induced apoptosis. Immunol Cell Biol. 2006;84(1):72-8.
33. Larimer BM, Bloch E, Nesti S, Austin EE, Wehrenberg-Klee E, Boland G, Mahmood U. The effectiveness of checkpoint inhibitor combinations and administration timing can be measured by granzyme B PET Imaging. Clin Cancer Res. 2019;15;25(4):1196-1205.
34. Bhattacharyya S, Tobacman JK. Interactions of CFTR and Arylsulfatase B (ARSB; N-acetylgalactosamine-4-sulfatase) in prostate carcinoma. Int J Mol Sci. 2025;26(9):4350.
35. Sharma G, Burke J, Bhattacharyya S, Sharma N, Katyal S, Park RL, Tobacman J. Reduced arylsulfatase B activity in leukocytes from cystic fibrosis patients. Pediatr Pulmonol 2013;48(3):236-244.

36. Bhattacharyya S, Tobacman JK. Increased arylsulfatase B activity in cystic fibrosis cells following correction of CFTR. Clin Chim Acta 2007;380(1-2):122-127.
37. Rao GJ, Christe ME. Inhibition of rabbit liver arylsulfatase B by phosphate esters Biochim. Biophys. Acta. 1984;788 (1): 58-61.
38. Wòjczyk B. Lysosomal arylsulfatases A and B from horse blood leukocytes: purification and physico-chemical properties. Biol. Cell. 1986; 57: 147-152.
39. Kotlo K, Bhattacharyya S, Yang B, Feferman L, Tejaskumar S, Linhardt R, Danziger R, Tobacman JK. Impact of salt exposure on N-acetylgalactosamine-4-sulfatase (arylsulfatase B) activity, glycosaminoglycans, kininogen, and bradykinin. Glycoconj J 2013;30(7):667-676.
40. Zhang X, Bhattacharyya S, Kusumo H, Goodlett CR, Tobacman JK, Guizzetti M. Arylsulfatase B modulates neurite outgrowth via astrocyte chondroitin-4-sulfate: Dysregulation by ethanol. Glia 2014;62(2):259-271.
41. Bhattacharyya S, Solakyildirim K, Zhang Z, Linhardt RJ, Tobacman JK. Chloroquine reduces Arylsulfatase B activity and increases chondroitin 4-sulfate: Implications for mechanisms of action and resistance. Malaria J 2009; 8(1):303.
42. Yang B, Bhattacharyya S, Linhardt R, Tobacman J. Exposure to common food additive carrageenan leads to reduced sulfatase activity and increase in sulfated glycosaminoglycans in human epithelial cells. Biochimie 2012;94(6):1309-1316.
43. Tzankov A, Bhattacharyya S, Kotlo K, Tobacman JK. Increase in chondroitin sulfate and decline in Arylsulfatase B may contribute to pathophysiology of COVID-19 respiratory failure. Pathobiology. 2022;89(2):81-91.
44. Bhattacharyya S, Tobacman JK. SARS-CoV-2 spike protein-ACE2 interaction increases carbohydrate sulfotransferases and reduces N-acetylgalactosamine-4-sulfatase by p38 MAPK. Signal Transduct Target Ther. 2024;9(1):39.
45. Bhattacharyya S, Feferman L, Tobacman JK. Restriction of aerobic metabolism by acquired or innate arylsulfatase B deficiency: A new approach to the Warburg effect. Sci Rep. 2016;6:32885.
46. Tessitore A, Pirozzi M, Auricchio A. Abnormal autophagy, ubiquitination, inflammation and apoptosis are dependent upon lysosomal storage and are useful biomarkers of mucopolysaccharidosis VI. Pathogenetics. 2009;2(1):4.
47. Roeser D, Schmidt B, Preusser-Kunze A, Rudolph MG. Probing the oxygen-binding site of the human formylglycine-generating enzyme using halide ions. Acta Crystallogr D Biol Crystallogr. 2007 May;63(Pt 5):621-7.
48. Roeser D, Preusser-Kunze A, Schmidt B, Gasow K, Wittmann JG, Dierks T, et al. A general binding mechanism for all human sulfatases by the formylglycine-generating enzyme. Proc Natl Acad Sci U S A. 2006;103(1):81-6.
49. Seo M, Qiu W, Bailey W, Criner GJ, Dransfield MT, Fuhlbrigge AL, et al. Genomics and response to long-term oxygen therapy in chronic obstructive pulmonary disease. J Mol Med (Berl). 2018;;96(12):1375-1385.
50. Bhattacharyya S, Solakyildirim K, Zhang Z, Linhardt RJ, Tobacman JK. Cell- bound IL-8 increases in bronchial epithelial cells following Arylsulfatase B silencing. Am J Respir Cell Mol Biol 2010;42(1):51-61.

Supplementary Figure Legends

Supplementary Fig.1. Effects of rhARSB treatment in other mouse melanoma models.

A. Treatment by rhARSB (0.2 mg/kg in ~40 µl saline) around the rim of B16F10 subcutaneous tumors in C57BL/6J mice was undertaken for 7 consecutive days in 7 female mice with measureable right flank melanomas. Previous work had treated with rhARSB preemptively on a fixed schedule, prior to the presence of measureable tumors. Initial procedures for tumor inoculation were similar to previous methods [5]. Survival was compared to 8 untreated mice which were treated with similar volume of normal saline at similar time points. Tumor volume was reduced by ARSB treatment at 6 of 7 time points ($p<0.05$, unpaired t-test, two-tailed, unequal variance). Survival was increased in the treated mice, from mean of 26 days in the controls to 31 days in the treated mice ($p=0.012$, log-rank test).

B. Immune-deficient female mice NSG™ humanized mice (NOD.Cg-*Prkdc*^{scid} Il2rg^{tm1Wjl}SzJ; strain #005557, Jackson Labs, Bar Harbor, ME) were engrafted with human PBMC and subsequently inoculated with 200,000 A375 human melanoma cells subcutaneously in the right flank. Treatment was rhARSB (0.2 mg/kg SQ at a concentration of 50 µg/ml saline) on days 2, 7, 14, 21, and 28 following tumor inoculation. Seven mice were treated with rhARSB, and 8 controls were treated with similar volume of saline on the same schedule. Mice were euthanized on day 31, when two of the untreated mice reached endpoint for tumor volume. All of the untreated mice had measureable tumors. In contrast, no tumors were palpable or visible in the treated mice.

Supplementary Fig.2. ARSB-induced effects on MMP expression in A375 cells by effects on IGF2R and c-Myc.

A,B. In A375 cells, the inhibitory effect of rhARSB on MMP9 and MMP2 expression was blocked by knockdown of the IGF2R (insulin-like growth factor 2 receptor), the mannose 6-phosphate receptor which enables uptake of rhARSB [4,13].

C. Overexpression of ARSB by specific plasmid had a similar effect on MMP2 and MMP9 expression as treatment by rhARSB. Overexpression was performed using ARSB plasmid in pCMV6-XL4 vector (OriGene, Rockville, MD) and introduced in A375 cells by transient transfection using 2 μg of the plasmid and Lipofectamine™ 2000 (Invitrogen, Thermo Fisher Scientific). Previously, controls included untransfected cells and cells transfected with empty vector control (OriGene). Media were exchanged after 6 h. Cells were incubated in a humidified, 37°C 5% CO_2 environment and harvested at 24 h after transfection. Effectiveness of transfection was determined by measurements of ARSB activity before and after transfection. ARSB activity was measured as previously reported [3,6].

D,E. Increases in MMP2 and MMP9 mRNA were inhibited by ERK activation inhibitor peptide 1, cell-permeable (ERKinh), p38-MAPK inhibitor (Ph), and c-Myc/Max inhibitor (F4; thiazolidinone) which blocks c-Myc-Max dimerization. Prior experiments in subcutaneous B16F10 melanomas and in cultured melanoma cells showed that ARSB affected the expression of MMP2 and MMP9 through SHP-2-mediated effects on phospho-ERK1/2 and subsequent effects on DNA binding of c-Myc [5,6]. Similar effects are shown in the A375 cells.

F. DNA-bound c-Myc was inhibited by treatment with rhARSB in A375 cells. Knockdown of IGF2R, which is required for cellular effects of exogenous rhARSB, inhibited this response [4,13].

G. ERK activation inhibitor peptide 1, cell-permeable (ERKinh), p38-MAPK inhibitor (Ph), and c-Myc/Max inhibitor (F4) blocked the increase in nuclear-bound c-Myc. ARSB siRNA increased DNA-bound c-Myc, and this increase was inhibited by ERK inhibitor, p38-MAPK inhibitor, and c-Myc/Max inhibitor (cell-permeable thiazolidinone, labelled F4), which completely suppressed the effect of ARSB silencing on DNA-bound c-Myc.

Supplementary Fig. 3. MMP expression modified by ARSB in other cell lines.

A. ARSB knockdown increased MMP2 expression in normal human melanocytes. The normal melanocytes were grown and treated as previously described [6,13]. Primary normal melanocytes were cultured in Airway Epithelial Cell Basal Medium (ATCC, Manassas, VA) with melanocyte

growth kit (ATCC) and maintained at 37°C in a humidified, 5% CO2 environment with media exchange every 3 days. Confluent cells were harvested by trypsin for primary cells (ATCC) and sub-cultured.

B. Consistent with other findings, rhARSB significantly reduced mRNA expression of MMP2 and MMP9 and ARSB siRNA significantly increased MMP2 and MMP9 expression in B16F10 mouse melanoma cells. There was greater increase of MMP2 than MMP9 by ARSB knockdown. B16F10 mouse melanoma cells were purchased (ATCC CRL-6475) and cultured in DMEM supplemented with 10% FBS and 1% penicillin-streptomycin. Cells were screened for pathogens by IDEXX BioAnalytics (Columbia, MO). Cells were maintained at 37°C in a humidified, 5% CO2 environment with media exchange every 2 days, and confluent cells in T-25 flasks were harvested by EDTA-trypsin, and sub-cultured.

Supplementary Fig.4. Cytokines/Chemokines following ARSB siRNA and rhARSB in A375 cells.

A. Inverse effects of rhARSB treatment vs. ARSB knockdown were evident in TNFα, VEGF, IL-6, and FGFβ in A375 cells. Cytokine array showed declines following rhARSB and increases following ARSB siRNA. RhARSB treatment increased IL10 in the A375 cells, consistent with the results in the B16F10 pulmonary melanomas.

B. mRNA expression data confirm the results of the cytokine array.

Supplementary Fig. 5. Binding of IL-8 with Chondroitin 4-Sulfate

A. Chondroitin 4-sulfate content in A375 human melanoma cells was reduced by rhARSB (1 ng/ml x 24h) and increased when ARSB was silenced by siRNA.

B. When rh IL-8 was added to wells of a 24-well plate coated with A375 cells, the amount of bound IL-8 declined when cells were treated with rhARSB and increased when ARSB was silenced, indicating that IL-8 binds more with more sulfated C4S present when ARSB is silenced. IL-8 in the cell extracts was measured by ELISA IL-8 (DY208, R&D Systems).

C. In an *in vitro* binding experiment, wells of a 24-well plate were coated with either C4S or C6S antibody (5 μg/ml) and C4S or C6S (100 μl; 2.5 μg/ml) was added. Subsequently, rhIL-8 at varying concentrations was added, biotinylated IL-8 antibody was added, and the extent of IL-8 binding detected by ELISA, as detailed in the Methods. Maximum binding of IL-8 with C4S was ~200 pg/ml. Virtually no IL-8 bound to chondroitin 6-sulfate.

D. When 250 pg/ml of IL-8 was added to wells coated with either C4S or C6S, 144.6 ± 11.7 pg/ml of IL-8 bound to C4S and 18.3 ± 3.2 pg/ml of IL-8 bound to C6S.

Fig.1. Impact of ARSB and Pembrolizumab and their combination on pulmonary metastases in B16F10 melanoma

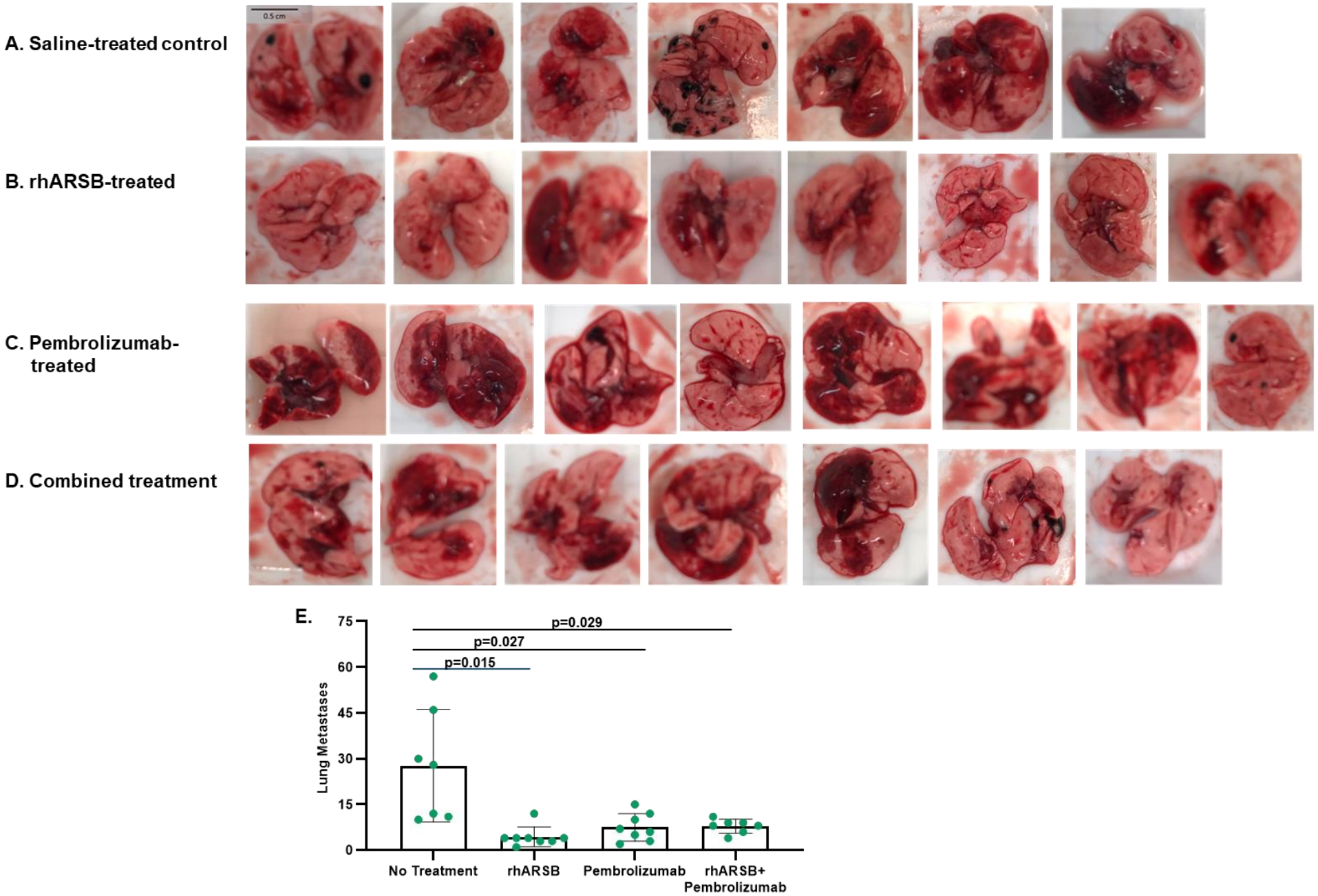

Fig. 2. Effect of Pembrolizumab and ARSB on COP1-mediated pathway of apoptosis in B16F10 pulmonary melanomas and A375 human melanoma cells

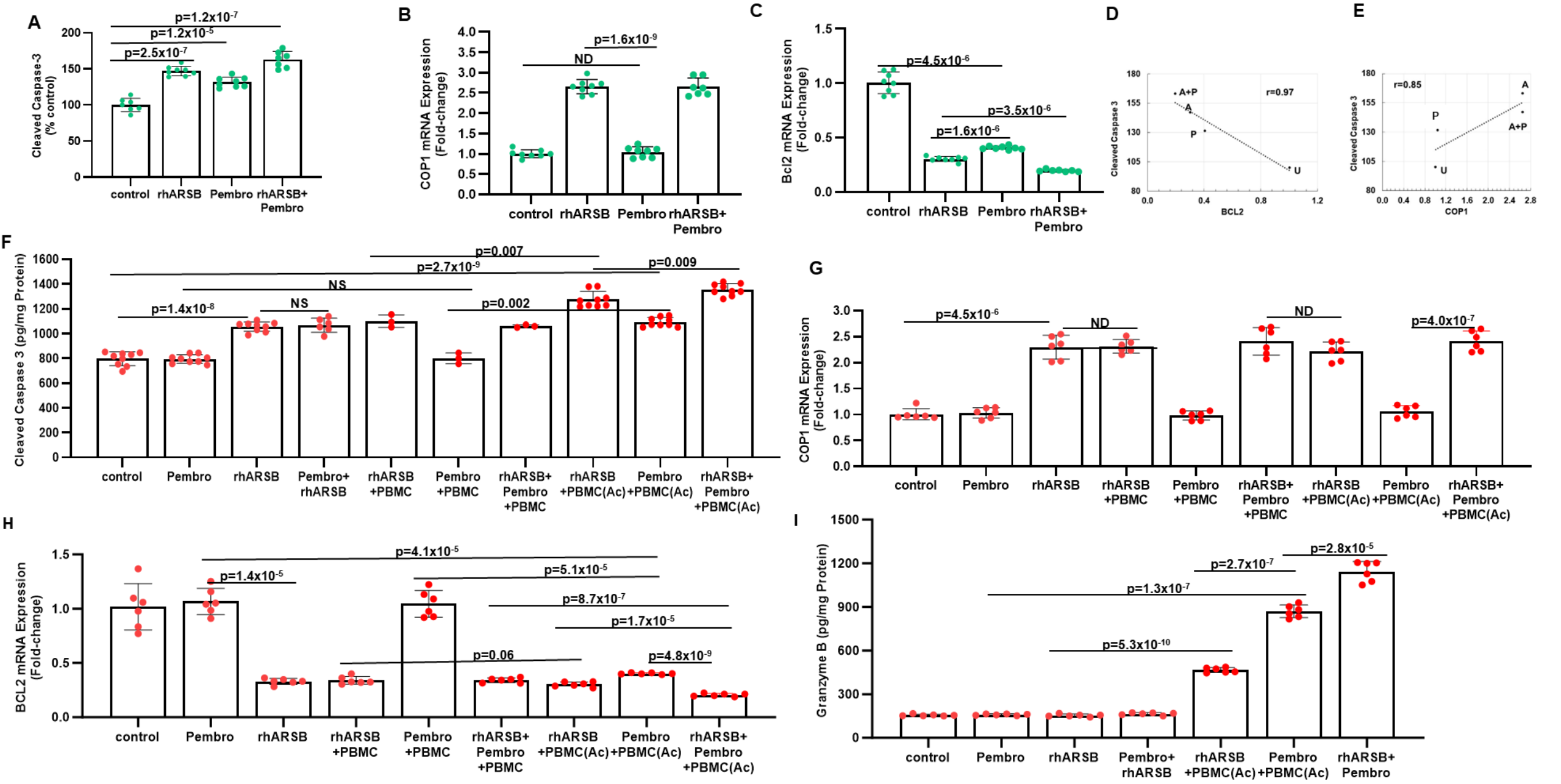

Fig.3. Matrix metalloproteinases following rhARSB and Pembrolizumab in B16F10 pulmonary metastatic melanoma and in A375 cells

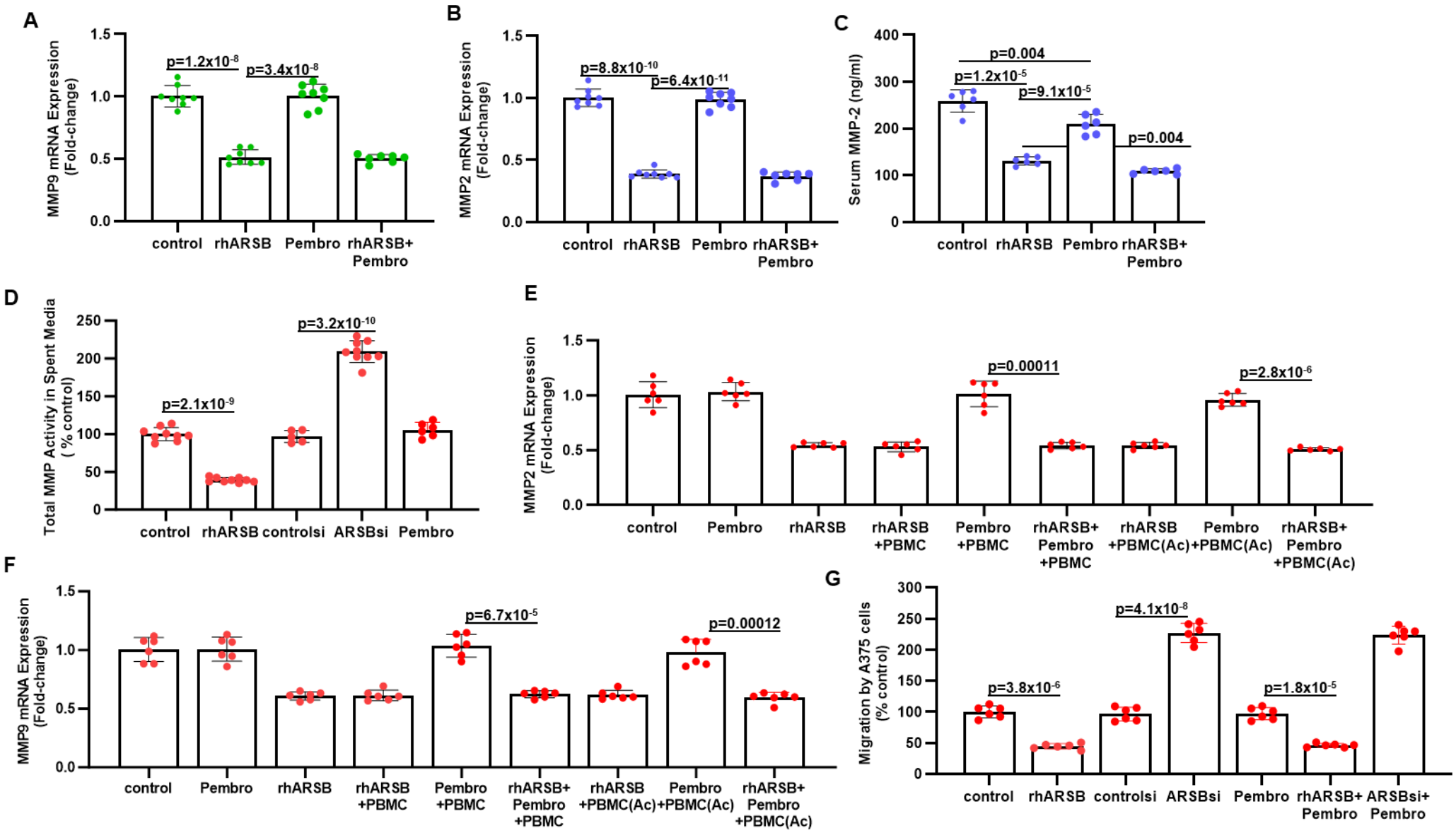

Fig.4. Expression of cytokines/chemokines in B16F10 melanoma lung tissue following rhARSB and Pembrolizumab

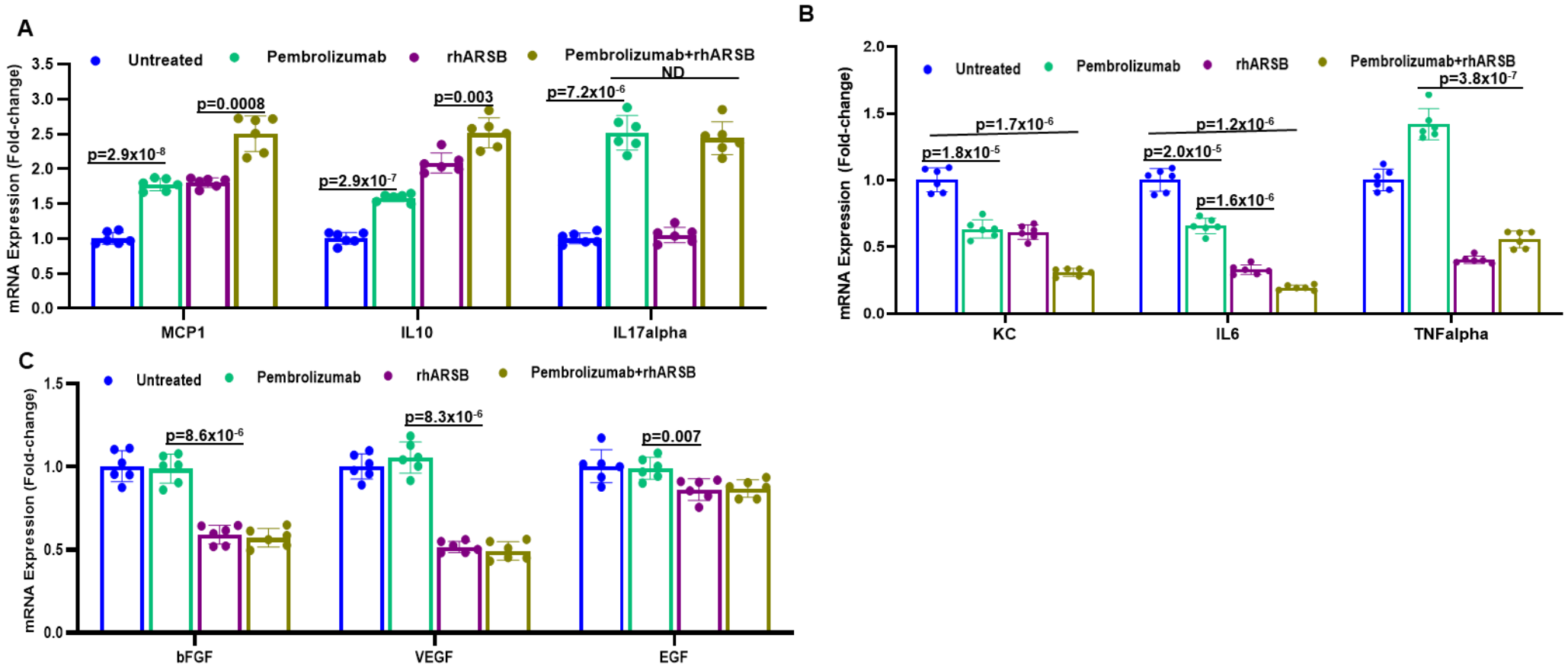
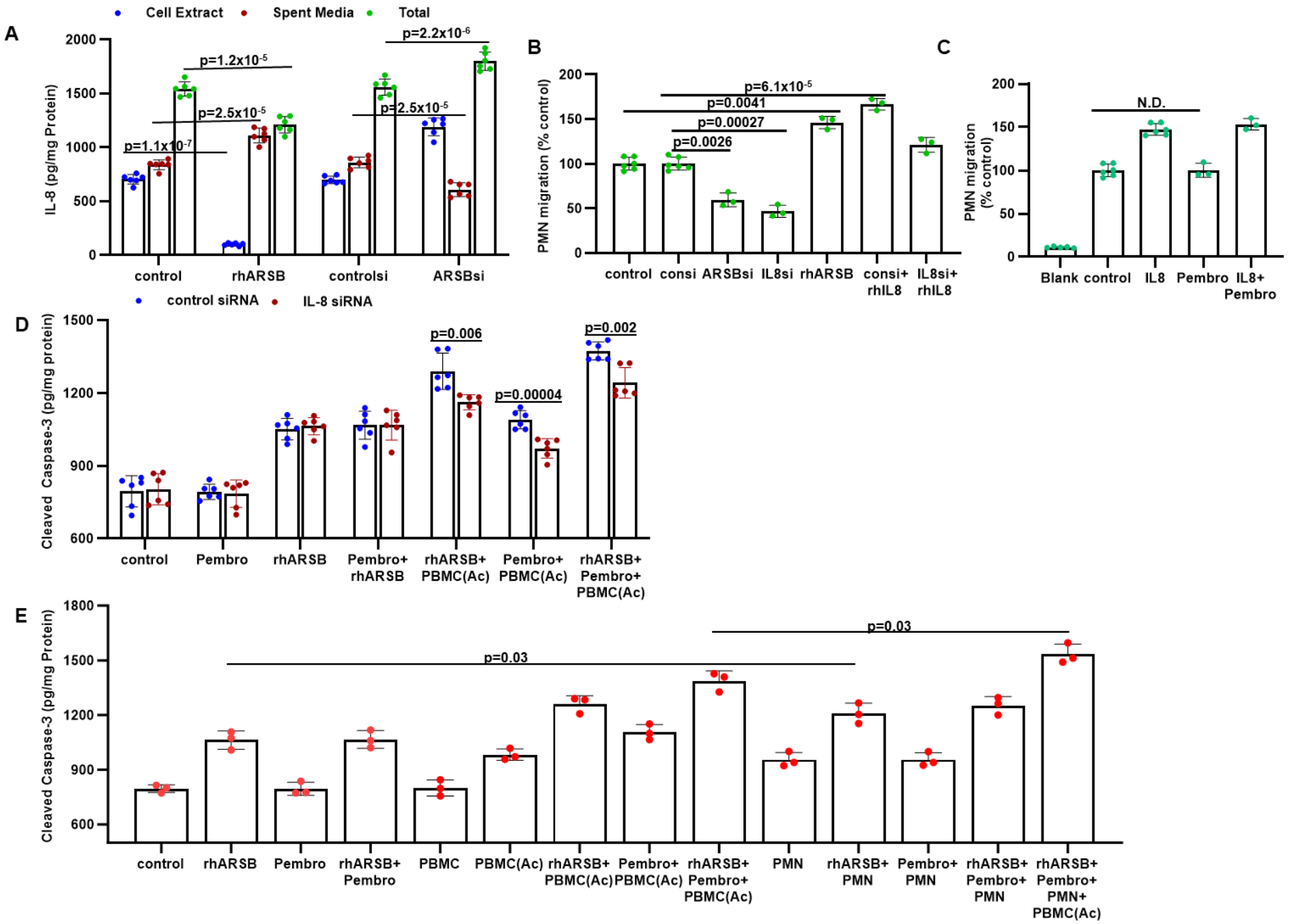
Fig.5. Effects of rhARSB and Pembrolizumab on polymorphonuclear (PMN) leukocyte invasion and apoptosis in A375 cells